HORIBA Scientific

Choose the fastest path to success

Research or OEM mass production

Why design a spectrometer system on your own, when HORIBA has highly experienced engineers, design tools and a broad range of pre-existing platforms to start from.

HORIBA Design/Engineering Teams for all components of an OEM system:

- Optical simulations (Concave grating spectrograph, Offner, Czerny-Turner, Dyson…)
- Mechanical design and CCD/CMOS sensor cooling
- Electronics/camera design
- From prototyping to performance validation & release

Your specifications and application requirements

You drive.
We design & deliver.

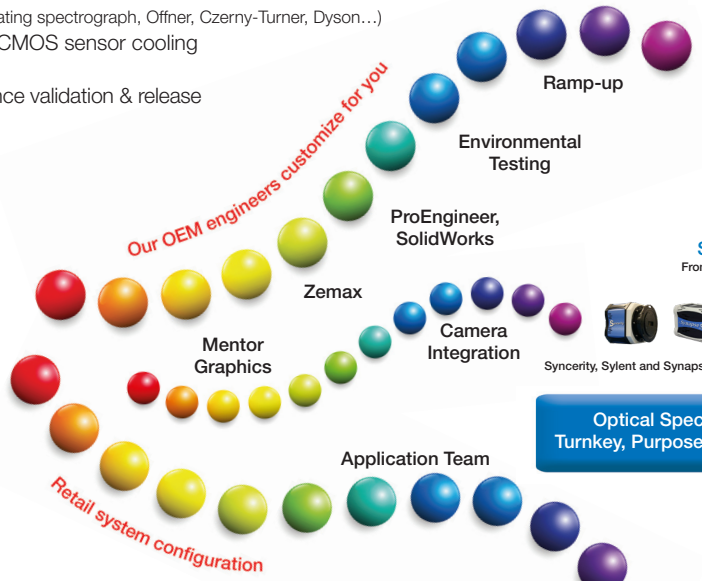

OEM: Customized Solutions for Industrial Volume Applications

Mass Volume Production

Spectroscopy & Imaging Cameras

From uncooled linear cameras to deep-cooled 2D cameras with CCD, EM, sCMOS or INGAAS sensors

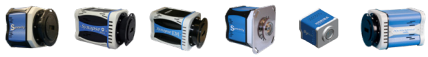

Syncerity, Sylent and Synapse cameras are designed and manufactured in New Jersey

Optical Spectroscopy Systems & Solutions: Turnkey, Purpose-built, Modular & Custom Solutions

Retail Solutions

HORIBA Retail Solutions from OSD (Optical Spectroscopy Division)
from standard spectroscopy components to turnkey custom systems

- Spectroscopy components such as spectrometers and deep-cooled CCDs
- Custom turnkey solutions for various spectroscopies
  - Raman • Reflectance/Transmittance • Dark Field Scattering • Electroluminescence
  - Photocurrent • Photoluminescence • PL Lifetime
- Full-featured software or software development kit (SDK, including LabVIEW™ VIs)
- Installation, service and experienced application support

horiba.com/OEM and **horiba.com/OSD** for more information

JOBIN YVON Technology

Focal Point Review

Applied Spectroscopy

Applied Spectroscopy
2017, Vol. 71(10) 2237–2252

DOI: 10.1177/0003702817720468
journals.sagepub.com/home/asp
SAGE

How to Design a Spectrometer

Alexander Scheeline

Abstract

Designing a spectrometer requires knowledge of the problem to be solved, the molecules whose properties will contribute to a solution of that problem and skill in many subfields of science and engineering. A seemingly simple problem, design of an ultraviolet, visible, and near-infrared spectrometer, is used to show the reasoning behind the trade-offs in instrument design. Rather than reporting a fully optimized instrument, the Yin and Yang of design choices, leading to decisions about financial cost, materials choice, resolution, throughput, aperture, and layout are described. To limit scope, aspects such as grating blaze, electronics design, and light sources are not presented. The review illustrates the mixture of mathematical rigor, rule of thumb, esthetics, and availability of components that contribute to the art of spectrometer design.

Keywords

Spectrometer engineering, absorption spectrometry, optical design, grating spectrometer, Fastie–Ebert spectrometer, spectrometer fit for purpose, plane grating spectrograph

Date received: 26 May 2017; accepted: 20 June 2017

Introduction

My graduate advisor, Professor John P. Walters, who had designed (or worked with others to design) several generations of spatio-temporally resolving optical spectrometers,[1–6] once advised me, "Never build your own spectrometer." Now that I and my collaborators have designed and built several spectrometers[7,8] and related optical systems,[9–12] I recommend to the reader: Never build your own spectrometer—unless doing so is the only way to solve a problem that you care about! But how can one know if the right instrument is already available from a vendor? One way is to design the ideal instrument for one's needs and then to go looking for that instrument in the marketplace. If something close is found, the user has confidence that it is right for the problem at hand. And if not? Then it is time to get a CAD package, a ray-tracing program, a compiler, or LabView (depending on one's programming psychology), an electronics text, and start engineering. As I was further taught by Professor Walters: Never be a slave to someone else's engineering. To that I only add, do not even be a slave to your own engineering. Break free and be creative!

Designing a spectrometer is a nonlinear process. It starts linearly:

(1) State the measurement problem.
(2) Determine the wavelength range, photometric precision, and resolution desired.
(3) Estimate available size, power, and financial resources.
(4) Devise optical parameters that meet the constraints of (1)–(3).
(5) Build and characterize the instrument.
(6) Make measurements and solve problems.

The reality is that after each step, it is likely that there will be some mismatch with constraints or goals. Perhaps resolution will be too high. Perhaps precision will be too low. Perhaps cost will be excessive. One then loops back to adjust some constraints in light of others. It is this dynamic back and forth among goals, parameters, and invention that makes a recipe for instrument design impossible (or at least unnecessarily confining). To illustrate instrument design, this paper shows one solution to a particular design challenge using technology available at a particular moment. Necessarily, some specific components from identified vendors are listed (and, at the end, we find that failure to choose a stock parameter value for one variable, mirror focal length, forces a choice between a custom

Department of Chemistry, University of Illinois at Urbana-Champaign, Champaign, IL, USA and Spectroclick Inc, Champaign, IL, USA

Corresponding author:
Alexander Scheeline, Department of Chemistry, University of Illinois at Urbana-Champaign, 600 S. Mathews Avenue, 461 RAL Box 48, Urbana, IL 61801, USA and SpectroClick Inc., 60 Hazelwood Dr., Champaign, IL 61820, USA.
Email: info@spectroclick.com

component and revising design parameters). These are not endorsements of the particular products; indeed, one expects that some desirable alternative product will be introduced while the manuscript is in press or immediately following publication. A useful exercise for the diligent reader who wants to become proficient at design is to retrace the design exercise and find alternative components to those listed here, or to redesign the instrument using a stock focal length for the collimator/camera mirror.

For those who would prefer a video rather than text, access this web link (which shows the design of the Czerny–Turner mount, and illustrates many of the ideas covered in this Focal Point).[13] For book-level depth, see Neumann's recent volumes.[14,15]

Before starting, it is recommended that the reader survey some of the standard textbooks and references on spectrometry and signal-to-noise (S/N) theory. Some of these are old, but their wisdom is not.[16–21] A reviewer suggested some YouTube videos to explain the Seidel aberrations; cited mini-lectures[22] may be helpful. Note that one of the citations is for a Fabry–Perot interferometer. How do you know you should be designing a spectrometer and not an interferometer? Only by knowing whether your problem of interest is in a regime where spectrometers "outperform" interferometers. The Ocean Optics wedge interferometer[23] is in competition with dispersive units for ultraviolet visible (UV–Vis) instruments, so wavelength region alone is no longer a basis for choice. My colleagues and I have previously published the design of an echelle spectrometer[7,24] whose performance has long since been eclipsed by a number of instruments, including the clearly described Varian instrument where a custom detector was part of the design.[25] Pelletier built a visible echelle for Raman spectroscopy.[26] Dovichi described a beautiful highly parallel low-resolution fluorescence spectrometer for DNA sequencing.[27] A massive literature on optimizing Czerny–Turner (plane grating) spectrographs exists and much of the knowledge and wisdom is summarized in a 1991 paper.[7] In the intervening quarter century, the improved ability to make aspheric mirrors has resulted in numerous ingenious designs including hypercorrected Czerny–Turners,[28] flat field spectrographs,[29] and Offner spectrographs.[30–32] The author's company recently released a handheld absorption/reflection instrument. Is there a general way to address why each of these instruments had different detectors, dispersers, focal lengths, and other design details? Let us address the various measurement aspects, explore ways to achieve them, and see how the components interact.

Determine Required Parameters

In the context of a specific problem, critical design parameters include:

(1) Wavelength, frequency, or energy range;
(2) Energy resolution;
(3) Temporal response;
(4) Available experiment time;
(5) Polarization characteristics of incident light and whether such polarization includes desired information (noting that polarization may influence signal, even if one is not interested in that information);
(6) Field of view;
(7) Spatial resolution;
(8) Necessary precision;
(9) Magnitude and spectrum of noise external to the spectrometer;
(10) Available signal and controls available for adjusting signal magnitude. These will have implications on noise as well as signal;
(11) Dynamic range of desired information;
(12) Mass, size, power, and connectivity available;
(13) Additional environmental constraints such as altitude, temperature, or humidity operating range.

Notice that there are no instrumental specifics at this stage, only measurement goals and environmental constraints. If, in mid-design, it becomes impossible to design an instrument that meets all the original criteria, one must revisit the constraints, relax some of them, and try again. For example, to get 0.01 cm^{-1} resolution, one either needs a wideband interferometer with 1 m mirror travel, a narrow band interferometer with high finesse, a grating spectrograph with high linear dispersion, or a narrowband, continuous wave laser. If one chooses the narrow band interferometer, some coarser wavelength resolution may be needed in series with the interferometer. But is 0.01 cm^{-1} the right resolution to solve a particular problem? There are some molecular spectroscopy problems (anything with resolution better than 0.3 GHz, i.e., looking for Lamb dips) where 0.01 cm^{-1} is too coarse. There are others (e.g., visible absorption by typical molecules in aqueous solution) where such high resolution is not only overkill but may actually prevent precise measurement of desired quantities due to insufficient light. Figure 1 gives examples of a spectrum with much important fine structure, what that spectrum would look like with 1 nm resolution, and then the spectrum of an aqueous dye where 1 nm resolution is excessively narrow.[33]

One must also consider engineering from several subdisciplines. Any modern instrument involves computer engineering or programming and design of the transductive interface between optical and electronic systems. Optical engineering is required to obtain the necessary image quality. Mechanical engineering and materials science are used together to obtain suitable mechanical, vibrational, and temperature stability. If solid or liquid samples are involved, chemical engineering, perhaps in the form of microfluidics, is a concern. If the instrument is particularly large or heavy, there may be civil engineering aspects (e.g., when the

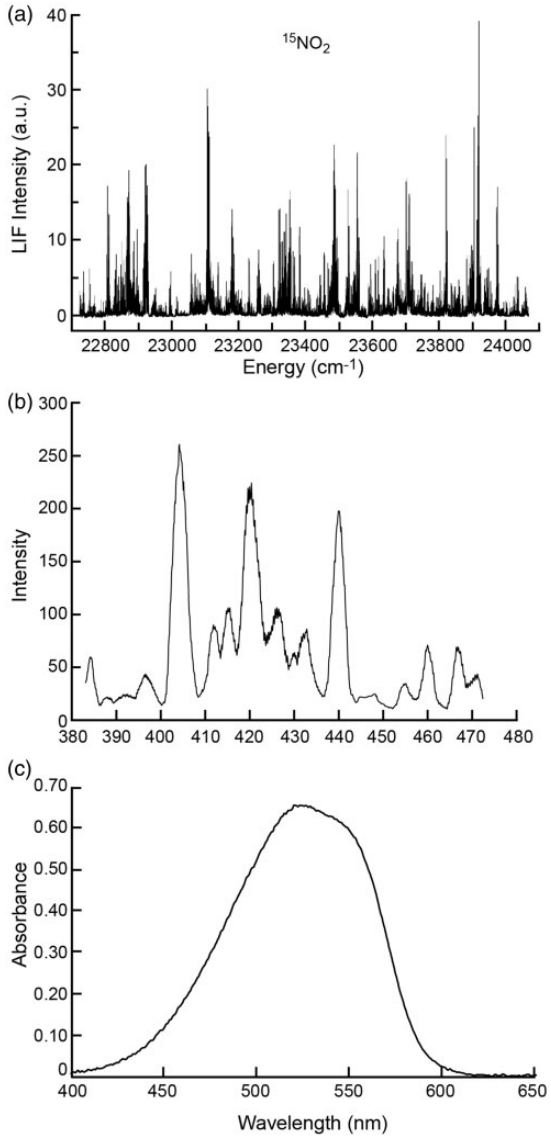

Figure 1. Examples of spectra with various optimum resolutions. (a) NO_2 laser-induced fluorescence with 0.1 cm^{-1} resolution.[33] (Copyright Elsevier, reprinted with permission.) (b) Simulation of NO_2 laser-induced fluorescence from inset (a) with 1 nm resolution, showing degradation from insufficient resolution. (c) Acidified Methyl Red with 1 nm resolution, showing lack of structure below ~10 nm.

National Institute for Standards and Technology was constructed, an entire room was dedicated to a 10.7 m (35 ft.) focal length normal incidence vacuum spectrograph. By comparison, my laboratories at the University of Illinois were 30 feet long (and 10, 20, or 30 feet wide), so such an instrument would have to fit diagonally into a room, taking into account safe entry/egress, air handling, and the ~70 ns round trip time from the entrance aperture to the focal plane). In many instances, one must also consider chemistry, sample preparation, species stability, photobleaching characteristics, and reactivity with air, solvents, and impurities.

To avoid turning this article into an overly lengthy tome, we will limit considerations to problems that can be solved using grating spectrometers and linear optical transitions (no wave mixing or intentional nonlinearity). We will ignore prisms, even though dispersion data on optical materials is more readily available now than ever before so that the non-constant dispersion of such systems is less of a problem than in prior decades. Note that any prism instrument design must account for imperfect repeatability in the composition and dispersion of the prism material. Those wishing to design with prisms may find the refractive index database webpage[22] to be a useful website.

Devise Parameters

Suppose spatial variability is not of interest; this means that hyperspectral imaging is unnecessary. As much light as one can collect needs to be transmitted through an entrance aperture into the spectrometer. It is important to remember the Law of Conservation of Etendue

$$\Xi = n^2 A\Omega \tag{1}$$

where Ξ is the etendue, n is refractive index, A is the area of the light beam, Ω is the solid angle of the beam.

For a point source, the emergent beam can be thought of as a cone with angle from normal to edge of θ_Ξ. The corresponding solid angle is $2\pi(1 - \cos\theta_\Xi)$. A hemisphere subtends 2π steradians. For small values of θ_Ξ, a series expansion of $\cos\theta_\Xi$ gives

$$\Omega = 2\pi\theta_\Xi^2 \tag{2}$$

In turn, for an optic with diameter d and distance from the light source f, the solid angle subtended is

$$\Omega = 4\pi\frac{\pi d^2/4}{4\pi f^2} = 4\pi\left(\frac{1}{4f/\#}\right)^2 \tag{3}$$

with $f/\#$ the ratio of the optic diameter to its distance from the object or focus. When $f/\#$ is specified for a lens or mirror, f is taken as the focal length of the optic, but in use the $f/\#$ varies. However, as shown in Fig. 2, because etendue is constant, attempts to increase throughput by decreasing image magnification are fruitless. Squeezing an image to a smaller area means increasing the solid angle, thus requiring a larger optic to capture all the light in the original beam. Thus, designing a spectrometer is a matter of knowing how much light is available, how much light fits the dynamic range of the detector, and choosing an $f/\#$ consistent with these constraints. Astronomical telescopes for looking at distant or weak objects typically have $f/\# < 6$, while those looking at great detail at closer objects have higher $f/\#$, allowing greater magnification but less throughput.

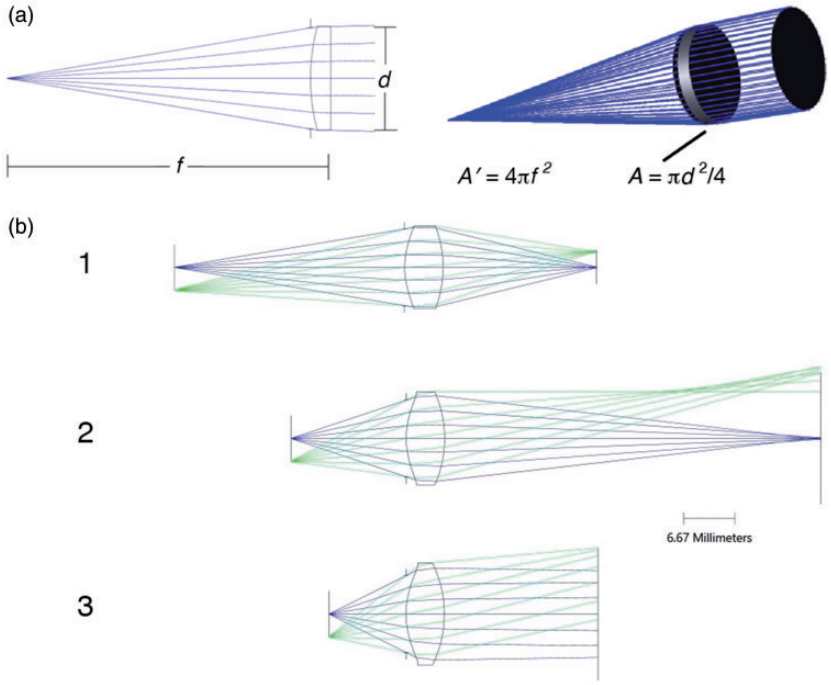

Figure 2. (a) Solid angle and *f*/#. A sphere of radius *f* has area $4\pi f^2$, while a lens of diameter *d* has an area of $\pi d^2/4$. (b) Conservation of etendue for aberration-free system. Lens has (unrealistically hyperbolic) first surface conic constant of -4.189 to cancel on-axis monochromatic aberrations. (b1) For $S_1 = 30$ mm, effective *f*/# = 3, included angle = 0.33 rad, and magnification = 1. (b2) For $S_1 = 15$ mm, effective *f*/# = 1.5, included angle = 0.644 rad, and magnification = 2.2. (b3) Lens focal length ~12.4 mm, *f*/1.24, planar included angle 0.767 rad (44°). Eq. 1 is approximately demonstrated; deviations are mainly due to the blur in (b2).

Before designing the dispersion system, one must decide among point detectors (photodiodes, photomultipliers), linear detectors (linear CMOS, linear charge-coupled device [CCD], diode array), or two-dimensional arrays (CCD, areal CMOS). Typically, for time resolution faster than one-30th of a second, point detectors or intensifier-gated arrays are required. If a point detector is employed, commonly there is an exit aperture to define wavelength resolution, and then the post-aperture beam expands to fill the detector aperture. For linear or areal arrays, the individual pixels or diodes serve as their own limiting aperture. Rarely can a single pixel or single diode be regarded as a resolution element. Suppose the spectrometer's dispersion resulted in a 0.01 nm line exactly filling one pixel. Then the slightest optical aberration, misalignment, or instrument vibration would send light from that line into an adjacent pixel. As a rule of thumb, one should allow three pixels for each resolution element in the absence of optical aberrations or image blur. Again, to maintain focus, we will not discuss the noise properties of detectors here, but such consideration is essential in computing signal, S/N ratio, and whether a particular detector is appropriate to a measurement (Fig. 3).

Ray tracing software is an essential tool for laying out an optical system. While a system can be roughed out using the paraxial approximation (all light makes only a small angle with respect to the shortest path from light source to detector)

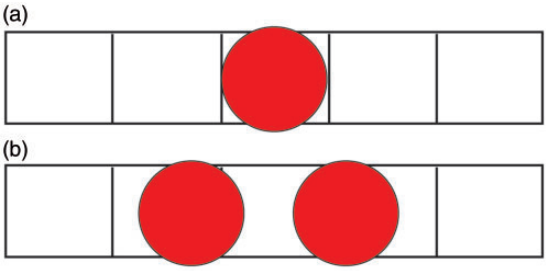

Figure 3. Pixel alignment versus entrance aperture size. (a) Perfect alignment of 1 nm effective width pixel with identical size, aberration-free entrance aperture. (b) Two signals, 1.5 nm apart, offset 0.5 nm from pixel-centered alignment. Middle pixel blurs data from the two optically resolved signals. To have two signals, 1 nm apart, free from overlap on any pixel, 1 nm must be dispersed across three pixels.

$$\frac{1}{S_1} + \frac{1}{S_2} = \frac{1}{f} \tag{4}$$

where S_1 is the distance from the entrance aperture to the collimating optic, S_2 is the distance from the focusing or camera lens or mirror to the detector or exit aperture, and

f is the instrument, lens, or mirror focal length, such simple design is inadequate for any realistic spectrometric system.

Aberrations such as spherical aberration, astigmatism, coma, and distortion/curvature all degrade images in ways that typically need to be compensated. All ray traces shown in this paper were done with Zemax Optic Studio v.14.2 (Zemax LLC). To find additional packages, do an internet search on "free ray trace software" without the quotation marks; both proprietary and open programs can be found from "hits" on the first page.

Resolution in wavelength must be translated into resolution or dispersion in space. When photomultipliers were the dominant detectors, the spectrometer exit slit width was usually the spatial parameter on which most calculation focused. In many modern instruments, array detectors are employed.[34] Suppose pixels have a width of *W* micrometers. Adjacent pixels may be contiguous or may have some small spacing, leaving an uncovered gap in spatial coverage of a dispersed signal. Such gaps are particularly likely for CMOS detectors since data conversion and clocking circuits may be interleaved with photosensitive areas. For simplicity, ignore such gaps. It is essentially impossible to exactly align a desired wavelength and resolution on a single pixel or column of pixels. While image blur and aberrations may make matters worse, it is almost always a good idea to allocate at least three pixel widths for one resolution element. If a resolution of 0.1 nm is desired, then each pixel should subtend no more than 0.03 nm in the dispersed spectrum. If the pixels are 2 μm wide, that means 0.1 nm should cover no more than 6 μm, for a dispersion of 16.7 nm/mm. However, this requires that the entrance aperture be only 2 μm wide. This is quite small, so throughput will be low. "Why not use a wider slit and demagnify the image?" Then the *f*/# must be high in the dispersing region of the instrument. For a 25 μm entrance slit to be demagnified to 2 μm requires demagnification of 12.5:1, so even if the final focusing lens or mirror is *f*/1 (a quite "fast" lens), the entrance aperture will be f/12.5 or slower (or else some of the light that comes through the entrance aperture will never reach the focal plane, thus being a source of stray light but not of useful information). Moral: big pixels are preferable to small pixels, though a desire for a compact detector may place an upper limit on pixel size. Because silicon can only store about 20 000 separated charges per square micrometer, big pixels have higher dynamic range. It is common for CCDs to have 13 μm^2 pixels that can store over one quarter million charges (and, yes, that is only about 2000 electrons per square μm, one order of magnitude smaller than the supposed maximum! Such conservative design favors linearity over maximum intensity dynamic range.). Diode arrays with rectangular pixels 25 μm wide and 2 mm high routinely can store over 10^8 electrons; it is this high charge storage ability and related high precision (up to one part in 10^4) that have recommended diode arrays for absorbance measurements since the early 1970s.

Table 1. Typical resolution in the UV and Vis spectral regions.

Measurement type	Typical resolution
Solution fluorescence (nm)	10
Solution absorption (nm)	1
Atomic absorption (resolution set by light source) (nm)[a]	1
Atomic absorption (resolution set by spectrometer) (nm)[a]	0.01
Atomic emission (nm)	0.01
Raman scattering (qualitative to match low resolution IR absorbance) (cm^{-1})	4
Gas phase absorbance or Raman scattering (cm^{-1})	0.1

[a]At first glance, the two starred resolution values appear backwards. Hollow cathode lamps have narrow line widths, while short focal length spectrometers have approximate nanometer resolution. The meaning here is that when the hollow cathode lamp sets resolution, one can employ a low-resolution spectrometer, while when one uses a continuum source, a high-resolution spectrometer is required.[40]

Once the detector geometry and dispersion are known, the focal length of the spectrometer and grating choice may be estimated. As rules of thumb, resolution can be chosen as shown in Table 1.

Because our earlier paper[7] ran through the trade-offs for atomic emission, here we will design an absorbance spectrometer. Any resemblance to a commercially available instrument is a consequence of the physics involved, not of dissection of any particular device. A 1 nm resolution means that three pixels in the focal plane should cover 1 nm. If the instrument is to cover from 200 nm to 900 nm, this means 900–200 = 700 resolution elements or $3 \times 700 = 2100$ detector elements. A quick Internet search resulted in finding a 2048 pixel CCD, the Excelitas RL2048P.[35] Since the point here is to show how to design and make trade-offs rather than to find the best possible components, we will design with this device. Important response and dimensional characteristics are given in Table 2.

The stunning lack of dark current specification is alas too common. Dark current increases exponentially with temperature. Typically for silicon, the dark current is 100 electrons s^{-1} for a 24 μm square pixel near room temperature, but see Widenhorn et al.[36] to learn why this number is a gross oversimplification. Assuming areal proportionality, the estimated dark current for the detector specified here is 34 electrons per pixel per second. Integration for ~1 s or less will mean that dark current is below the amplifier noise level, while longer integration will result in dark current shot noise being less important than gradual dynamic range compression from the integral of the current.

Why must the detector be specified in this detail? We know that at 600 nm, we can only tolerate a little less than

Table 2. Characteristics of the Excelitas RL2048P linear CCD.

Characteristic	Value	Characteristic	Value
Minimum wavelength (nm)	200	Signal per electron (μV)	6.6
Maximum wavelength (nm)	1000	Dynamic range	> 2500
Pixel width and height	14 × 14 μm	Peak quantum efficiency	0.9 @ 600 nm
Saturation charge (electrons)	167 000	Readout clock (ns/pixel)	25
Amplifier noise (electrons)	50	Dark current	Not mentioned
Saturation voltage (V)	1.1	Cover window	Quartz

167 000 photons per second/quantum efficiency = 185 000 photons per second on a 14 μm square pixel. This will inform how much light may or must enter the instrument and will interact with choices about the size of the entrance aperture. Also note that we are 52 detection elements short of being able to cover the full 700 nm range we specified. We have to choose whether to slightly sacrifice resolution or slightly sacrifice wavelength range. Let us play two hunches: (1) most spectral features are sufficiently wide that a slight sacrifice in resolution will not matter; and (2) optical aberrations will slightly degrade resolution in any event. The result will be that nominal dispersion should be 700 nm across 2000 pixels, each 14 μm wide or 700 nm / 28 mm or 25 nm/mm. The entranced aperture will be no more than 14 μm in diameter (to avoid blurring between pixels), and may be smaller if the full 14 μm entrance aperture supplies too much light.

How do we achieve 25 nm/mm dispersion? For a diffraction grating illuminated at normal incidence,

$$n\lambda = d\sin\beta \tag{5}$$

where n is diffraction order (integer), λ is a wavelength at which constructive interference/full visibility occurs, d is the spacing of any regular structure such as grooves, modulations, or refractive index variation occur in the grating, and β is the diffraction angle.

The use of d for spacing is unfortunate, as it is easy to confuse with the d used in differential calculus. The literature has used this convention for over a century, so it cannot be avoided.

Angular dispersion is

$$\frac{d\lambda}{d\beta} = \frac{d}{n}\cos\beta \tag{6}$$

The position of a wavelength in the focal plane, x, is proportional to spectrometer focal length f and off-axis angle β (in radians). In fact, saying $x = f\beta$ is a small angle approximation. More accurately (for a spectrometer with a planar focal surface normal to the central ray propagating at $n = 0$),

$$x = f\tan\beta \tag{7}$$

Because many spectrometers work at small off-axis angles (and our design instrument here will work with $n = 1$ and β small), we use the small angle approximation and

$$\frac{d\lambda}{dx} = \frac{d\cos\beta}{nf} \tag{8}$$

or even (since cos $x \sim 1$ for small x),

$$\frac{d\lambda}{dx} = \frac{d}{nf} \tag{9}$$

In low dispersion situations, $n = 1$ is commonly used. In addition to permitting a more comfortable (longer) focal length than would be possible for the desired dispersion in higher orders, $n = 1$ gives the widest possible free spectral range (wavelength range without overlap of shorter wavelengths at $n > 1$). At the position where $\lambda = 400$ nm for $n = 1$, all gratings will also have $\lambda = 200$ nm for $n = 2$. Blocking this order overlap will require attention later, but we note it here to ensure that the problem is floating just below the surface for the rest of the design. Prisms do not suffer from order overlap. They do, however, suffer from low dispersion in the red region of the spectrum and nonlinear dispersion throughout the spectrum. While modern computing makes the nonlinear dispersion a less important nuisance than in the early years of photoelectric spectrometry, the poor dispersion can only be overcome by using multiple prisms for different, perhaps overlapping, wavelength ranges, resulting in mechanical complexity.

Inserting $n = 1$ in Eq. 9, 25 nm/mm = d/f. For a 1200 line/mm grating (commonly available from a variety of vendors), $d = 1/1200$ mm = 833.3 nm so $f = 33.333$ mm. Is this likely to work? If incident light is normal to the grating, 833.3 nm light will diffract parallel to the grating surface ($\beta = 90°$) so 900 nm light will only occur in zero order. What about a 300 line/mm grating (also common)? Now $d = 3333.3$ nm and f is 138.9 mm. Recall that the 2048 element detector is 28 mm long. Figure 4 sketches the implications for instrument geometry if we chose this grating. Initially, we ignore refraction effects in the window overlaying the detector. From Eq. 5, $\beta(200\text{ nm}) = 3.44°$ and $\beta(900\text{ nm}) = 15.66°$. This places the first detector element

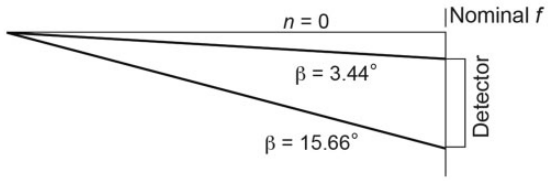

Figure 4. Putative geometry for a 300 line/mm grating, 14 μm/pixel 2000 element linear detector with first approximation dispersion 25 nm/mm.

at $x = 138.9 \tan(3.44^\circ)$ mm = 8.35 mm from zero order and the last detector element at 8.35 + 28 = 36.35 mm from zero order.

An additional problem with the above design is that 138.9 mm is a non-standard focal length. The closest common focal lengths are 5 in. (1/8 m) or 6 in. (152.4 mm). While a custom focal length is of course possible, it is expensive unless a design is to be mass produced. Choosing a slightly shorter focal length will reduce resolution but relax the precision with which the array detector must be positioned. With a 125 mm focal length and 300 groove per mm grating, nominal dispersion is 26 2/3 nm mm^{-1} for a nominal resolution of 1.12 nm.

Unfortunately, this simple geometrical argument does not fully explain observed spectra. If the instrument is laid out with a concave grating, illuminated along its normal (the Paschen–Runge mount[37]), the focal "plane" is the Rowland circle; the linear detector position shown above is approximately at the sagittal focus of this grating and astigmatism ensures that wavelengths blur together. If we move to the Rowland circle itself, where wavelengths are cleanly and optimally resolved, the focal "plane" is the surface of a sphere so that only two wavelengths are in best focus. If we use a holographic grating designed to distort the diffracted wavefront to optimally focus on a planar detector, we then need to design and fabricate that grating, and any custom grating, even planar, is expensive. The reason concave grating spectrometers can be inexpensively obtained is that replica holographic gratings can be cloned from a master or mass produced *en batch* economically. To avoid getting bogged down in the design of such gratings,[38,39] we will work with plane gratings so we can emphasize specification of *f*/# and entrance aperture, optical aberration minimization, dimensional precision, and optical coatings for dealing with order overlap.

What *f*/# should we employ? Rule of thumb reflectance of a mirror is 95% and grating efficiency is 50% (though much higher efficiency for a sharply blazed grating is possible; for example, Richardson Grating Lab[40] shows a 300 lines per mm grating with peak efficiency 80% and exceeding 40% between 300 and 800 nm). To get 185 000 photons per second on a 14 μm square detection element at 500 nm thus requires an entering flux of $185\,000/(0.95^2 \times 0.5) = 4.1 \times 10^5$ photons/s through the entrance aperture within the light cone seen by the mirrors. Suppose the deuterium lamp and incandescent filament sources used in common spectrometers are each $(10\text{ mm})^2$. At unity magnification, the entrance aperture will admit $(0.014\text{ mm})^2/(10\text{ mm})^2$ of the generated light. Suppose the filament emits 10 W with a blackbody radiation temperature of 3000 K and an emissivity of 0.8 (typical of tungsten). Then the total flux through the entrance aperture is $0.0014^2 \times 10 \times 0.8 = 1.57\,\mu$W. Looking up the blackbody curve,[41] we see 390 pW/sterad at 500 nm. Recalling that each pixel sees approximately 1/3 nm, we can see in Table 3 how much light will reach the detector. Power to photon count conversion comes from Planck's Law:

Table 3. Approximate illumination of $(14\,\mu\text{m})^2$ pixel at 500 nm as a function of *f*/#.

f/#	Solid angle (sterad)	Power (pW)	Photons s^{-1} at 500 nm	Time to saturate pixel (ms)
2	0.196	76	1.95×10^8	2
4	0.049	19	5×10^7	8
8	0.012	4.7	1.25×10^7	33
16	0.003	1.2	3.1×10^6	132

$$P = Nh\nu = \frac{Nhc}{\lambda} \tag{10}$$

where *P* = power in Watts, *N* = number of photons per second, *h* = Planck's constant, $\sim 6.626 \times 10^{-34}$ J s, *c* = speed of light, $\sim 2.997 \times 10^8$ m s^{-1}.

Since the array can only read out 30 times per second (once per 30 ms), there is no compelling reason to use a system faster than f/8. Such a slow system should limit aberrations and reduce the need for aspheric optics. 125 mm/8 ~ 16 mm; the optics can be small (5/8" diameter). In fact, one might well decide to build a Fastie–Ebert spectrometer (one mirror serves for both collimation and focusing) rather than a Czerny–Turner (two separate mirrors) unless the focal plane is too highly curved. The diameter of the beam collimating optic needs to match the diameter of the grating.

Why is filling the grating with light critical? Recall that the highest relative resolution ($\lambda/\Delta\lambda$) that can be realized by an unaberrated instrument with infinitely small pixels is *nW*/*d*, the order number times the width of the grating divided by the line spacing, or the order number times the number of illuminated grating lines. If the grating is underfilled, one is paying for (and mechanically supporting) a critical component which is underutilized. Overfilling leads to excess stray light. Illuminating the grating in converging or diverging light also reduces realizable resolution. Properly illuminating the grating is worth considerable effort in optimizing the design. However, this raises another issue. What is the

relative resolution desired in the visible region of the spectrum? For 1 nm operating resolution, allowing for some degradation by other components in the instrument, perhaps 0.5 nm resolution by the grating is adequate. If the longest wavelength employed is 900 nm, then that means $\lambda/\Delta\lambda = 1800$, and the grating need have no more than 1800 lines illuminated. For a 300 line/mm grating, that is a grating 6 mm wide. At *f*/8, we specified that the optical beam is 16 mm wide, bigger than the limit required but not excessive. Were we designing an instrument for atomic spectrometry, where relative resolution of 50 000 is desirable, it is clear that a finer grating, larger in size, working in higher orders would be desirable.

Now that the "back of the envelope" design is done, we proceed to layout, simulation, and optimization.

Detailed Design, Assembly, and Characterization

We will design the system as simply as possible. A Fastie–Ebert[42,43] system could have a pinhole entrance aperture above the grating, the linear array below the grating, and the grating rotated about an axis parallel to the pinhole/grating axis. Since the same mirror is used for collimation and focusing, the design is tightly constrained as shown in Fig. 5. The simplest and least expensive realization has the single collimator/camera mirror spherical. As in the classic Jarrell Ash 3.4 meter Ebert spectrograph used for many years for atomic emission work, the next improvement is to use a parabolic mirror. Are either of these adequate? Is a parabola overkill? Is the image curvature noted in the original design of importance here? Should the entrance aperture and detector be placed at the circle of least confusion, the tangential focus, or the sagittal focus of the mirror? Ray tracing is the simplest way to decide such critical parameters.

Because a spectrograph is an imaging system containing a dispersing element, the first approximation requires imaging to be optimized with a plane mirror substituting for the diffraction grating. Choose a spherical mirror with radius of curvature 250 mm (focal length 125 mm). Offset the entrance slit 11 mm from a normal to the center of the mirror, masking the mirror with an aperture 16 mm in diameter (125 mm/16 mm = *f*/7.5)[a]. The plane mirror (or, later in design, grating) is centered on the concave mirror normal, reflecting the (nearly) collimated beam to a point on the mirror centered 11 mm on the other side of the normal, and focusing to a point symmetrically on the opposite side of the mirror normal. The angle between the entering ray to the mirror/pseudo grating and the mirror normal is 5.04 °. The ray trace is in Fig. 5 and includes a spot diagram of the focus going through the plane whose distance from the mirror equals the distance of the entrance aperture (numerically optimized at 124.94 mm). This mimics the behavior described for the Czerny–Turner system by Goldstein and Walters.[19,20] The circle of least confusion has a diameter of about 32 μm. As individual pixels are 14 μm wide, the blur amounts to 32/14 = 2.3 pixels. Until we see what off-axis aberrations do to resolution, it is premature to judge if the circle of least confusion blur is a problem. We do note, however, that the tangential (leftmost through-focus spot diagram) and sagittal (rightmost through-focus spot diagram) foci have widths of ~10 μm, smaller than the detector pixels, and thus will not degrade resolution.

Which way should the grating pivot so that the spectrum is cleanest? If the grating rotates about the *x*-axis as shown in Fig. 6, the wavelength will disperse perpendicular to the plane of the page and the focus resolving spectra will be cleanest in the sagittal focal plane. If rotated about the *y*-axis (as is normally done with a Czerny–Turner instrument), the focus will be best in the tangential plane. In either case, we must be alert to the possibility that the cleanest spectra will not have the detector mounted perpendicular to the ray from the focus mirror to the detector (as intimated in Fig. 4). The center of the detector should correspond roughly to 550 nm. This corresponds to $\beta \sim \arcsin(550\text{ nm}/3333.33\text{ nm}) = 9.5^\circ$.

First, we disperse the spectrum normal to the plane of the "W" pattern of collimation and focusing. Fig. 6a (side view) and 6b (top view) are the result. On a whole-instrument scale, the dispersion is beautiful – close to a straight vertical line and all wavelengths in focus. Close examination shows the spot diagrams at 100 nm wavelength intervals in Fig. 7a. From 350 nm to 750 nm, no spot is wider than 40 μm or 3 pixels. Outside of this wavelength range, comatic blur increases to 65 μm at 250 nm, 4.5 pixels. The imaging is astonishingly good—better than I had anticipated when choosing the example. What if the grating is rotated about the *y*-axis as is typical in a Czerny–Turner design? As shown in Fig. 6c, the image quality is irrelevant because the dispersed spectra are, for half the wavelength range, reflected back to the grating rather than being transmitted to the detector. This is solved in the case of the Czerny–Turner layout by canting the camera mirror at an angle steeper than the entrance mirror, but this is not an option for the Ebert design.

An examination of Fig. 6 shows that the rays between the mirror and the focal plane come close to the diffraction grating. In laying out the instrument, one must guard against rays striking components that scatter light from the light beam or block part of the beam. Such *vignetting* reduces throughput and dramatically increases stray light. If the vignetting component is the grating, additional diffraction orders appear. Such *re-entrant spectra* are confusing at best and fatal to spectral purity at worst.

The non-Gaussian, asymmetrical line shape means that a simple equation for resolution as a function of wavelength cannot be written. Philosophically, the resolution is the root mean square (RMS) resolution generated from each

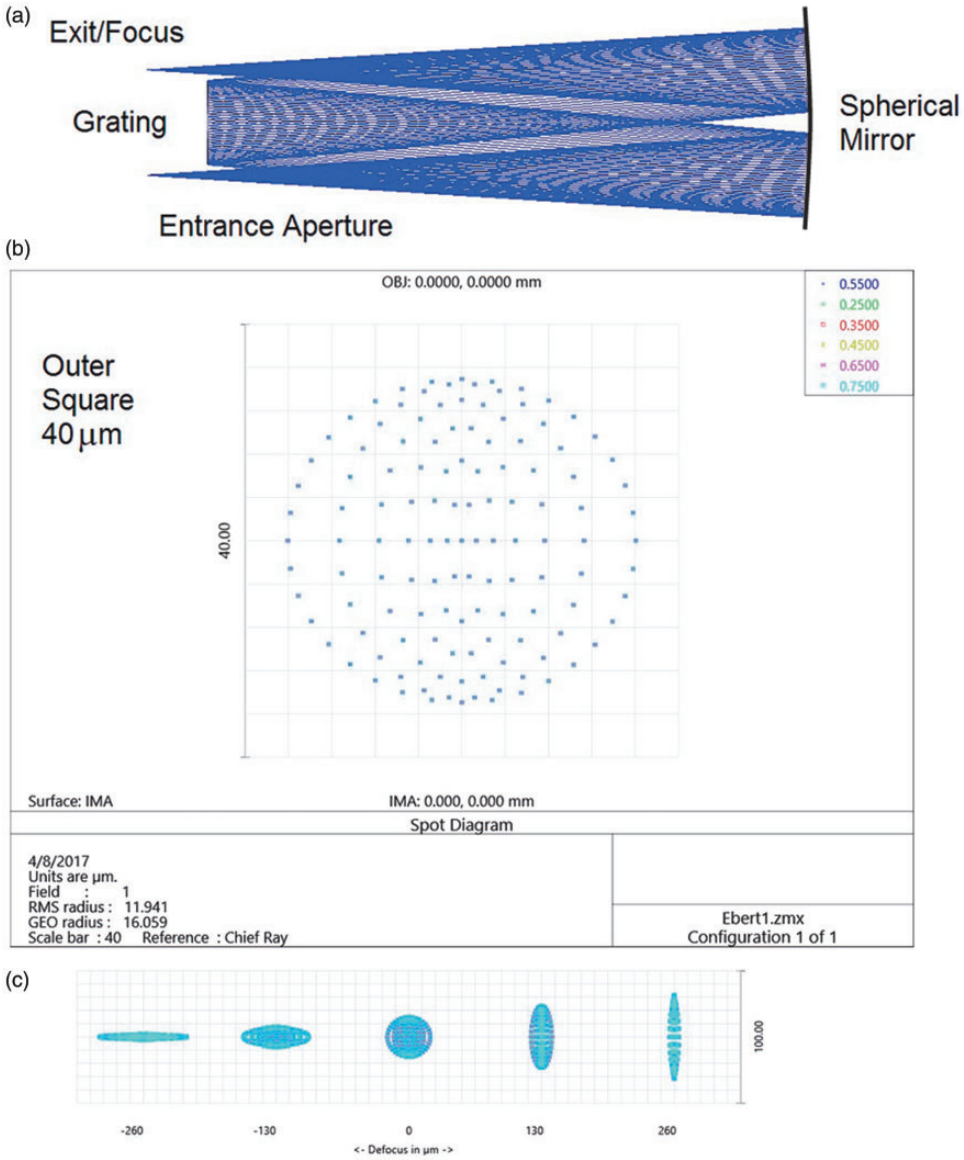

Figure 5. Fastie–Ebert spectrograph with grating replaced by a mirror. (a) Ray trace showing symmetrical image from illuminating sections of a spherical mirror centered 11 mm away from the axis (125 mm focal length). (b) Spot diagram of the circle of least confusion. (c) Spot diagrams moving through focus, with 130 µm step between images chosen so that tangential and sagittal foci are visible.

of the limiting components, grating, detector pixel size, entrance aperture, and optics

$$\sigma_{total} \geq \sqrt{\sigma^2_{entrance} + \sigma^2_{grating} + \sigma^2_{pixel} + \sigma^2_{imaging}} \qquad (11)$$

Rather than trying to devise a formula taking into account the shape of the entrance aperture, width of the sinc^2 function from the number of illuminated grooves and order of the grating, size of each pixel, and comatic blur, examination of spot diagrams can suggest the width and skew of the light coming from each wavelength and thus the shift, cross-talk, and reduction in throughput due to optical aberrations.

Changing to a parabolic mirror changes optical aberrations, but the side view of the ray bundles changes little. The optimum distance for the entrance aperture from the mirror becomes 125.3 mm, only a 330 µm change (I chose optimization ignoring lateral chromatic aberration, which meant only the focus at 550 nm contributed to the optimization). Astigmatism is unchanged, but coma does change. One can also optimize the conic constant of the mirror. For a sphere, the constant is 0. For a parabola, the constant is −1. The optimum for this design turns out to be −1.403, slightly hyperbolic. Spot widths in the direction of dispersion (the only blur that matters for resolution, given the square pixels of the linear detector) are as given in Table 4. Blur perpendicular to dispersion influences

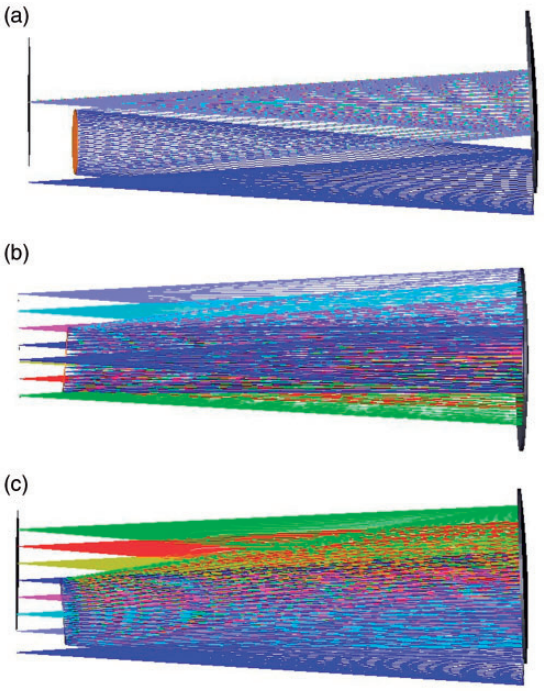

Figure 6. Ebert spectrometer layout. (a) Ray trace perpendicular to grating dispersion. Dispersed rays fall along a vertical line out of the plane of the figure. (b) Dispersion perpendicular to azimuthal plane. Corresponding image quality shown in Fig. 7. (c) Consequence of trying to use in-plane dispersion in the manner of a Czerny–Turner spectrograph. Rays in (b) do not intersect the grating, as they pass behind it; rays in (c) do intersect the grating. Despite clean spectral behavior (not shown), re-entrant spectra (dispersed spectra reflected back to the grating and then redispersed) make the design wholly impractical. Here, only wavelengths shorter than 500 nm avoid reentrance. Color code: green = 250 nm, red = 350 nm, tan = 450 nm, dark blue = entering, combined beam and 550 nm, aqua = 650 nm, violet = 750 nm.

throughput, which is considered later. RMS blur is the radius of a circle inside of which is 67% of all light at the given wavelength. When optimizing, I arbitrarily said $S_1 = S_2$, i.e., the distance from the entrance aperture to the mirror and from the mirror to the detector had to be equal. Small improvements in imaging could be obtained without this assumption. However, from the standpoint of building an instrument, having a single reference surface against which to attach the entrance aperture and the detector likely outweighs any small imaging improvement when one is aiming for reasonable manufacturing costs.

Comparing the numbers for the spherical mirror and the spot diagrams in Fig. 5c, it is obvious that looking at numbers without looking at ray traces can give an overly optimistic picture of how the spectrometer operates. Comparing parabolic and optimal mirror performance, it is clear that the significant additional cost of making a hyperbolic mirror compared to a parabola is only worthwhile at wavelengths beyond 750 nm. Astonishingly, the spherical mirror, when considered over the entire wavelength range, gives more uniform performance than the parabolic or optimal mirrors (in no case is blur in the wavelength-dispersing direction worse than five pixels, and while the RMS blur is bigger in mid-spectrum than for the optimized conics, the performance away from spectrum center is less degraded).

Not obvious from Table 4 is that the coma that gives rise to much of the blur also subtly shifts the position of the focused wavelength asymmetrically. Thus, in addition to blurring the image, coma results in slight shift in dispersion and spectral calibration. A good example is for the spherical mirror case at $\lambda = 250$ nm. While the image height is small ($<40\,\mu$m), it is stretched to 65 μm with most of the blur pointing to shorter wavelengths. The light is dispersed onto the correct nominal pixel and four more to the blue of the nominal pixel. Doubtless one could model the blur and, given sufficient measurement precision, correct for it, but such correction is to the author's knowledge rarely performed in low end spectrometers. One simply reads intensity pixel by pixel and ignores subtle blurring and calibration errors.

What about throughput? The blur means that less light falls on each pixel than we predicted when we discussed *f*/#. A pixel 14 μm square has the same area as a circular pixel with radius 7.9 μm. Each pixel sees $\pm 0.4\ r_{RMS}$ to the extent that the comatic blur is circular. As the ray traces show, the blur varies along the spectrum. At 550 nm, about half of the light from a given wavelength falls on a single pixel. Adjacent wavelengths illuminate the pixel, so dynamic range is only slightly sacrificed. Towards the red end of the spectrum, as little as one-sixth of the light from a single wavelength hits the nominal pixel expected to detect that wavelength.

It is at this point that design refinement truly begins. We have a not-too-bad design, but is it good enough to solve the problem we are interested in? Does the blur give an unacceptable amount of stray light from adjacent wavelengths? Does the blur reduce resolution and throughput unacceptably? If we try to increase throughput by going to a lower (faster) *f*/#, aberrations will be a bigger problem (the blur will be worse). If we try to reduce aberrations by going to a longer focal length and operating at a higher *f*/#, then throughput will be reduced and integration times extended, perhaps requiring cooling of the detector to avoid integrating too much dark current. Further, to fit the dispersed spectrum onto the same detector, an even coarser grating would be required. For 250 mm focal length, a 150 line per mm grating would give the same dispersion as the 300 line per mm grating did at 125 mm focal length. Further, the instrument would be bigger. From Table 4, we know that optical blur is no more than five pixels, so a resolution element is no more than seven pixels, meaning true resolution is no worse than 26 2/3 nm/mm $\times$ 7 $\times$ 0.014 mm = 2.6 nm. If that is good enough, the basics of the design are

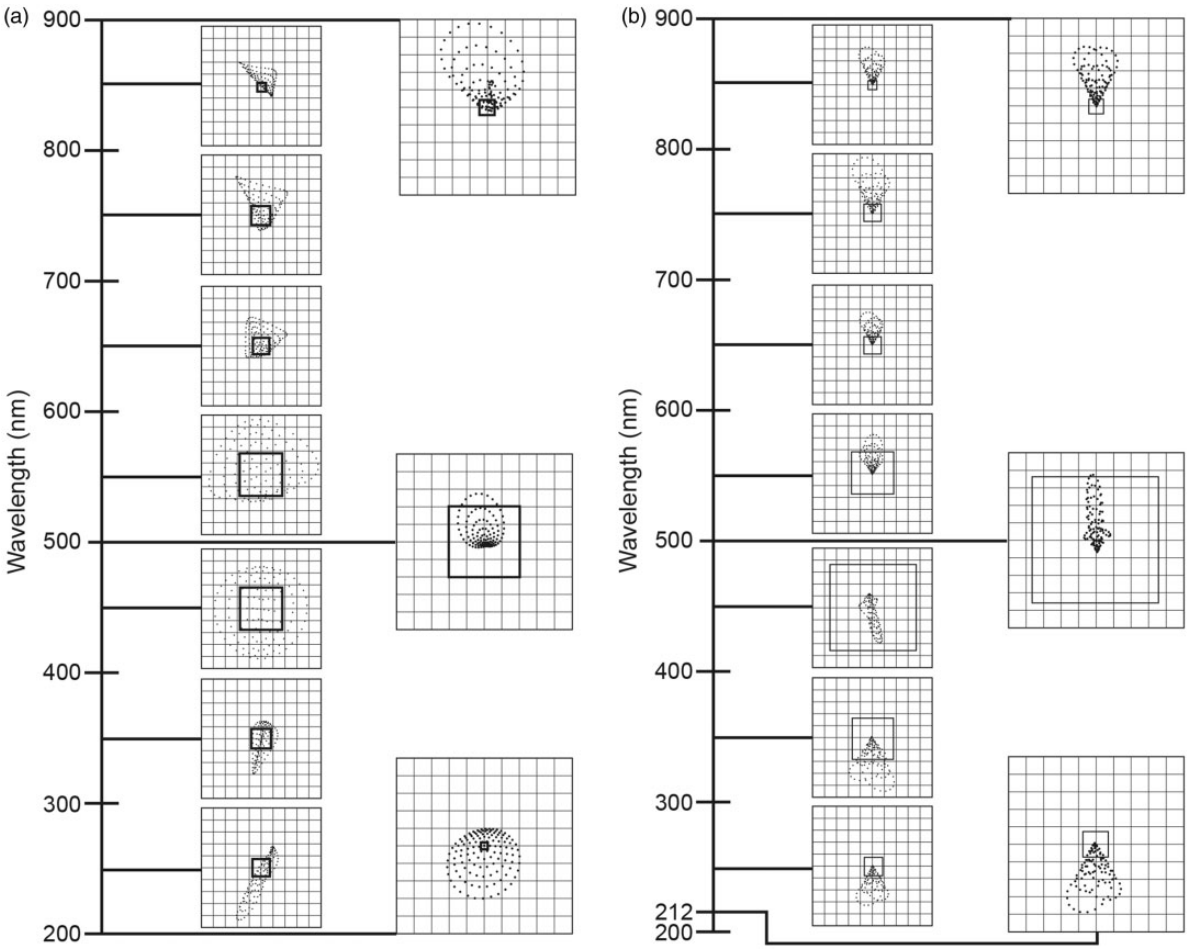

Figure 7. Spot diagram showing image quality from Ebert spectrometer. Square in each inset corresponds to 14 μm^2 pixel. (a) Using spherical mirror and no field-flattening lens. (b) With hyperbolic mirror and field-flattening lens. Note how the symmetrical spot at mid-image is distorted as well as defocused towards the ends of the spectrum. This influences resolution, throughput, and wavelength accuracy. Inset (b) requires more numerous and expensive components, but increases throughput and more symmetrically skews comatic blur away from the 500 nm center of the spectrum.

Table 4. Blur in dispersion direction for each of three mirror configurations and RMS blur of image spot. All blur is in micrometers. Note: Optimal mirror does not include a cylindrical lens in front of the detector; for that improvement, see Table 6.

	Spherical mirror		Parabolic mirror		Optimal mirror (conic constant—1.403)	
Wavelength (nm)	In dispersion direction	RMS radius	In dispersion direction	RMS radius	In dispersion direction	RMS radius
250	65	20.4	140	48.4	130	48.5
350	45	14.1	70	26.6	60	25.4
450	30	12.0	35	10.7	26	8.8
550	28	12.2	17	6.85	14	6.17
650	35	13.8	27	13.3	28	13.7
750	45	17.8	40	19.1	50	21.4
850	60	25.3	230	25.9	80	32.4

Table 5. Offset of optimum focus from detector plane for initial design. All distances show how far behind the plane the focus is found.

Wavelength (nm)	Best focus offset from Euclidean plane (μm)
250	750
350	500
450	200
550	0
650	0
750	100
850	300

Table 6. Imaging change if detector is covered with a cylindrical lens, planar on the side facing the detector and radius of curvature 41 mm on the side facing the incoming light.

	Image size (μm)	
Wavelength (nm)	In dispersion direction	RMS radius
250	33	15.4
350	18	8.4
450	9	2.7
550	13	5.6
650	28	12.4
750	45	20.1
850	62	28.6

done and the next steps can begin. If one needs sub-2 nm resolution across the spectrum, a longer focal length, slower *f/#*, lower throughput design is warranted. Alternatively, one can work with a more complex design, i.e., a Czerny–Turner mount (where the collimator and camera mirrors need not be concentric) or an enhanced Czerny–Turner mount in which a third mirror is added as a field flattener and aberration modifier (per Princeton Instruments' IsoPlane design[28]).

Why is the focus, as shown in Fig. 7a, not better? If we look through the focal plane, we can see that field curvature moves the optimum focus away from a Euclidean plane. To one significant figure, the offsets from that plane are as shown in Table 5.

How might we generate a wavelength-dependent increase in path length so that we can move the foci closer to the Euclidean plane of the detector? A cylindrical lens, thinner towards the edges of the detector, should work. In setting up this optimization, a glitch forced a minor alteration: the minimum wavelength for which Zemax allows silica to be employed in an optical system is 210 nm. Thus, we substitute 212 nm for 200 nm in the following variant of the instrument design. We continue to allow for a non-spherical mirror. Following optimization, the conic constant optimum is −1.334 or, effectively, −4/3. The effect of the cylindrical lens and hyperbolic mirror gives focal performance as shown in Table 6 and Fig. 7b. Compare the image size parameters with those in Table 4. Except at wavelengths longer than 700 nm, the improvement is obvious. At 300–600 nm, all the light hits the active area of detector pixels, and up to 700 nm, at least half the light falls on active detector pixels. No focus is more than four pixels high, meaning no less than one-12th of the light at each wavelength falls on the correct pixel. Thus, except at 850 nm where performance is unchanged, performance is significantly improved. Is this the limit of improving resolution and throughput? No. One can now design and, thanks to single point diamond turning, fabricate free form lenses. A toroidal lens with aspheric surfaces in both directions could further sharpen the image. One might even design a holographic lens where internal refractive index gradients substitute for curved surfaces. The cost, however, would be significantly greater than a simple cylindrical lens. If mass production were envisioned and the capital cost spread over hundreds of thousands of units, such subtle and sophisticated improvements might be plausible. For a single instrument, it is doubtful such optimization would be cost effective. After all, what has been designed here is already available commercially for less than $5000; we are designing an alternative to illustrate the process, not to compete! To summarize the design, see Table 7.

"We know where all the parts go. Aren't we done?" Alas, no. How precisely must the parts align for performance to remain adequate? Over what temperature range must the system operate? It is common for users to worry about the temperature's influence on the detector, recognizing that higher temperature means higher dark current. But temperature also influences wavelength calibration, alignment stability, focus precision, and intensity stability. Are the mechanical clearances adequate? The detector has width, height, and thickness; are these compatible with the space available given the optical geometry? If the space is inadequate, so that a steeper entrance angle is required (moving the entrance aperture and detector farther apart), is resolution preserved? How will the grating be mounted, and will the angle be adjustable? Adjustability allows for calibration of each instrument individually, relaxing requirements for part precision. However, adjustability likely increases drift and ensures that calibration is required. Further, adjustability adds complexity and cost. And then there are subtleties of the real components as opposed to idealized components. How will we modify the detector to avoid order overlap, and what is the effect of the quartz cover plate protecting the detector? The cover plate acts to foreshorten the focal distance. A 1 mm-thick quartz plate has an optical thickness of refractive index

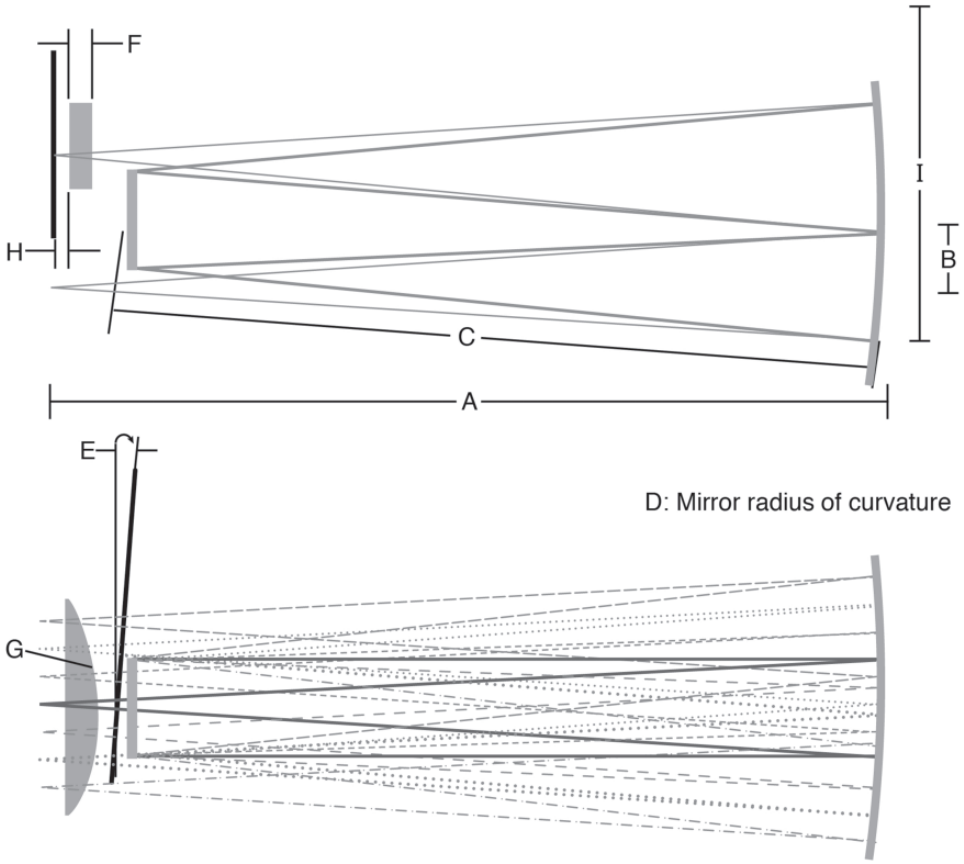

Figure 8. Dimensions quantified in Table 7.

Table 7. Design distances as transcribed from optimized Zemax ray traces using a spherical mirror. Dimensions labeled in Fig. 8

Dimension	No cylindrical lens	With cylindrical lens
A. Entrance aperture to mirror (mm)	125.4	124.7
B. Grating center to entrance or exit axes (mm)	11	11
C. Mirror intercept to grating center	113.8	113.8
Mirror conic constant	0	–4/3
D. Mirror radius of curvature (mm)	250	250
Grating ruling (lines/mm)	300	300
E. Grating rotation angle (°)	8.9	8.9
Detector rotation about *x*-axis (°)	−3.04	0.16
F. Cover plate thickness (mm)	–	3 at center
G. Cylindrical lens radius in *x* direction (mm)	–	41
H. Cover plate/detector gap (mm)	–	1
I. Mirror diameter (mm)	50	50
Grating size (square) (mm)	10 × 10 × 3	10 × 10 × 3

times 1 mm, a wavelength-dependent quantity that varies from 1.5505 mm at 200 nm to 1.4517 mm at 900 nm. To optimize focus across this range, the detector may need to be canted slightly from being perpendicular to the optical axis, and anywhere away from the meridional plane of the instrument, incident rays will trace a zigzag path within the cover plate as they reflect from air/quartz interfaces. As shown in Fig. 9, for an incidence angle of θ_i, Snell's Law says the beam will propagate at an angle of $\sin^{-1}(\sin\theta_i/n(\lambda))$ interior to the cover plate. A single traverse of the cover plate offsets the beam towards the θ_i=0 axis by $\sim d\tan(\sin^{-1}(\sin\theta/n(\lambda)))$, where d is the thickness of the cover plate. For 5° incidence, the offset is 59 μm at $\lambda = 500$ nm. A round-trip (double reflection) path gains an additional offset of $\sim 2d\tan(\sin^{-1}(\sin\theta/n(\lambda))) = \frac{2d\sin\theta/n(\lambda)}{\sqrt{1-(\sin\theta/n(\lambda))^2}} 2\mathrm{d}\sin\theta/n(\lambda)$, which for 5° incidence angle is ~120 μm. Refraction displaces the image by approximately four pixels, subtly changing wavelength calibration, and also spills 0.1% of the light an additional nine pixels farther along the detector. Anti-reflection coating of the cover plate minimizes lateral transfer of multiply reflected light, and can even be used to help suppress order overlap. Coating of the detector behind the cover

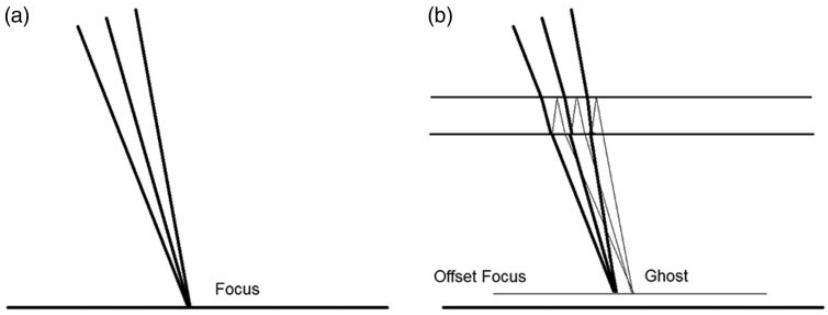

Figure 9. Effect of detector cover plate on converging beam, incident at an angle. Insertion of the cover plate above the detector/focal plane shortens the focus and generates ghost images for non-normal incident rays.

plate with a fluorophore may help with UV sensitivity by shifting UV light to the green or red, wavelengths at which silicon is more sensitive. However, some fluorescence scatters back towards the mirror, giving rise to stray light.

Dealing with the non-idealities of each component is tedious but essential to understanding instrument performance and limiting its degradation. For example, for the specific detector we have chosen, the cover plate is 0.5 mm thick. At normal incidence, the cover plate acts as a Fabry–Perot interferometer with mirror reflectance ~4% and free spectral range of 1.46 cm^{-1}. For broadband applications, such modulation is irrelevant. For atomic spectrometry, it might be significant. We have already seen that removing the planar cover plate and replacing it with a cylindrical lens improves performance and avoids fringing effects. To deal with order overlap, the cover or detector pixels must be coated with a thin film filter that blocks wavelengths below 200 nm starting near the pixels detecting 390 nm (two-sevenths of the way across the detector), additionally blocking below 300 nm starting near 590 nm (just beyond mid-detector), blocking below 400 nm starting near 800 nm (the last seventh of the detector). Filter fabrication is available from numerous vendors, but getting masking, adhesion, and performance in variably humid environments to be consistent is challenging, particularly when production quantities are small so that setup charges are a significant fraction of fabrication cost. Inserting the cover plate moves the optimum focus by plate thickness times (refractive index −1) or about 0.45 mm per millimeter of quartz or silica in the cover plate. This seemingly small distance is critical; we saw in Fig. 5c that detector and entrance plane positioning must be accurate to better than ±130 μm (Arrak[44] showed that a 2.25 m spectrograph had to be focused within ±0.5 mm to get intensity accurate within 10%, which proportionately scales to ±28 μm for a 0.125 m instrument).

Mirror and lens thin film coating is important to maximize throughput and minimize the sorts of ghosts already discussed for windows. Bare aluminum reflects well in the visible but poorly in the UV. Magnesium fluoride overcoating enhances aluminum reflectivity in the UV, but is hygroscopic and can cloud in humid atmospheres. Most optical houses can recommend broadband overcoating to cover various spectral regions, but in a situation such as we designed here, where UV and visible are both needed simultaneously, coating choice is more difficult.

Table 8. Coefficient of thermal expansion and implications for spectrograph temperature stability.[45]

Material	Coefficient of thermal expansion (μm/m/K)	Change in length of 125 mm base for 1 °C (μm)	Change in length of 125 mm base for 20 °C (μm)
Aluminum	21–24	3	60
Steel	11–12.5	1.5	30
Invar	1.5	0.2	4
		Change in length of detector array for 1 °C (nm)	Change in length of detector array for 20 °C (μm)
Silicon	3–5	86	1.7

If we ignore dimensional changes in mirrors and gratings (unwise, but a useful simplification when illustrating the problem), focal drift with temperature depends on the coefficient of thermal expansion (CTE) of the spectrometer frame or housing. For three common materials, typical CTE is shown in Table 8.

Given the sensitivity of the instrument to defocusing, we can see that Invar is necessary for the very best stability, but an aluminum frame is adequate for use in heated, air-conditioned spaces (nearly constant temperature). Stability is further improved if the gratings and mirrors are made of materials that expand so as to slightly reduce dispersion as temperature increases and the base lengthens (thus maintaining focal clarity and pixel alignment).

What about vibration sensitivity? At low frequencies, the entire spectrometer vibrates as a unit. At high frequencies, inertia damps mechanical motion. In between, various

components vibrate with specific mechanical resonances. If the usage case exposes instruments to frequencies corresponding to the resonance of a grating or mirror, spectra will blur, though phase-locked detection (uncommon in array detectors but common for photodiodes and photomultipliers) may be able to minimize the influence of the blurring. Vibration immunity is a consideration that rarely affects the research scientist but typically does affect the applications scientist. Vibration isolation tables became common in the 1970s and are readily procured from multiple vendors, but are frequently too awkward for field use. Benchtop instruments (or vehicle-born instruments) thus must avoid having resonances that correspond to such stimulae as fans, harmonics of the electric grid frequency (different in North America than elsewhere), building frame resonances stimulated by footsteps or passing traffic, or other mechanical devices such as nearby lathes or milling machines. One can imagine field instruments that could resonate from the bellow of a farm animal.

Even if all of these influences are considered, parameter tolerances, or part-to-part variation, must be considered. Optics frequently are centered with a precision of 0.1 mm, and have focal lengths precise to 0.5%. Tighter tolerances add to cost. For single-instance instruments, having adjustability to tune out the effects of component imprecision may be viable, but for production instruments adjustments must not require user attention. Which is better—a spectrometer with 0.1 nm resolution for perfect matching between design parameters and execution, but with a variation from instrument to instrument of 1% in dispersion, or an instrument with 0.5 nm resolution and 0.5% dispersion variation? At 500 nm, the former instrument has an uncertainty of 5 nm for calibration of a given pixel, while in the latter case the uncertainty is 2.5 nm, and in neither case is the nominal instrument resolution accurate without external calibration. Ray tracing software typically allows modeling of tolerance precision.

Conclusion

The steps to designing a compact Ebert spectrometer for UV–Vis–near-infrared (NIR) spectroscopy have been traversed. Left ambiguous was whether the improved resolution and throughput of the hyperbolic mirror/aberration correcting lens design was worth the significantly increased cost. A hyperbolic mirror is likely a custom design. Even with single point diamond turning, this is likely a $1000 or more component. Thorlabs lists either 100 mm or 150 mm focal length, 50 mm diameter spherical mirrors for less than $100 as stock items, but we designed for 125 mm focal length (and it was only while drafting this conclusion that the lack of 125 mm focal length as a stock item came to the author's attention). "So change to a standard focal length." To maintain wavelength coverage requires changing the grating, which likely means a custom design for that component. Sticking with 300 lines per mm, one has to choose between sacrificing 25% of wavelength coverage (longer focal length) or 25% of resolution. Deciding whether to optimize for part availability, cost, resolution, or throughput, is a matter of the specific measurement problem. "Why didn't you start, knowing what standard focal lengths are available? Now we have to start over?" In fact, iterating the steps demonstrated here, discovering additional constraints, and continuing to iterate until a workable design is completed is exactly what spectrometer engineering entails. At some point, one may know enough about a design to approach a vendor, knowing quite precisely whether an instrument will perform at the desired level. The reasons various instruments cost what they do will be evident, so that even if you do not build your own instrument, both you and your vendor will be likely to be less frustrated because constraints can be clearly explained and trade-offs communicated.

Conflict of Interest

The authors report there are no conflicts of interest.

Funding

This research received no specific grant from any funding agency in the public, commercial, or not-for-profit sectors.

Supplemental Material

All supplemental material mentioned in the text, consisting of the Zemax files for the various design stages for the spectrometer, is available in the online version of the journal.

Note

a. This offset is chosen so that entering and exiting rays miss the grating by a few millimeters but off-axis angles are as small as feasible. If a greater offset is chosen, the grating position will move closer to the mirror and farther from the entrance aperture and focal plane. Coma would be worse at higher offset.

References

1. J.P. Walters. "A Plane-Grating Time-Resolved Spectrometer for Basic and Analytical Emission Spectrometry". Anal. Chem. 1967. 39(7): 770–780.
2. J.P. Walters. Investigations into the Analytical Uses of Time-Resolved Spark Spectroscopy. A Study of the Sampling Step in the Point-to-Plane Spectrochemical Analysis of Aluminum Base Alloys. [Ph.D. Thesis]. Urbana-Champaign, IL: University of Illinois, 1965.
3. R.D. Sacks, J.P. Walters. "Short-Time, Spatially-Resolved Radiation Processes in a High-Voltage Spark Discharge". Anal. Chem. 1970. 42(1): 61–84.
4. R.J. Klueppel, D.M. Coleman, W.S. Eaton, S.A. Goldstein, et al. "A Spectrometer for Time-Gated, Spatially-Resolved Study of Repetitive Electrical Discharge". Spectrochim. Acta, Part B. 1978. 33B(1–2): 1–30.
5. J.P. Walters. The Heath Monochromator. https://web.archive.org/web/20050330151247/http://www.stolaf.edu/people/walters/narrative/mono.html [accessed Jan 1 2016].

6. R.J. Klueppel, D.M. Coleman, W.S. Eaton, S.A. Goldstein, et al. "Spectrometer for Time-Gated, Spatially-Resolved Study of Repetitive Electrical Discharges". Spectrochim. Acta, Part B. 1978. 33(1–2): 1–30.
7. A. Scheeline, C.A. Bye, D.L. Miller, S.W. Rynders, et al. "Design and Characterization of an Echelle Spectrometer for Fundamental and Applied Emission Spectrochemical Analysis". Appl. Spectrosc. 1991. 45(3): 334–341.
8. A. Scheeline, T.A. Bui. "Stacked, Mutually Rotated Diffraction Gratings as Enablers of Portable Visible Spectrometry". Appl. Spectrosc. 2016. 70(5): 766–777.
9. J.C. Cabalo, J. Schmidt, J.O.L. Wendt, A. Scheeline. "Spectrometric Systems for Characterizing Drop and Powder Trajectories and Chemistry in Reactive Flows". Appl. Spectrosc. 2002. 56(10): 1345–1353.
10. A. Scheeline. "Teaching, Learning, and Using Spectroscopy with Commercial, Off-the-Shelf Technology". Appl. Spectrosc. 2010. 64(9): 256A–268A.
11. B.J. Mork, A. Scheeline. "Observations of High-Voltage Atmospheric-Pressure Spark Discharges in Argon Using a Charge-Coupled Device Detector". Spectrochim. Acta, Part B. 1989. 44(12): 1297–1323.
12. B.J. Mork, A. Scheeline. "Wavelength-Resolved Single-Spark Emission Images Using a Charge Coupled Device Detector". Appl. Spectrosc. 1988. 42(8): 1332–1335.
13. A. Scheeline, A. Ibarra. How to Build a Czerny–Turner Spectrograph. https://ensemble.illinois.edu/Watch/spectrograph [accessed Jan 1 2016].
14. W. Neumann. Fundamentals of Dispersive Optical Spectroscopy Systems. Bellingham, WA: SPIE Digital Library, 2014.
15. W. Neumann. Applications of Dispersive Optical Spectroscopy Systems. Bellingham, WA: SPIE Digital Library, 2015.
16. J.D. Ingle, S.R. Crouch. Spectrochemical Analysis. New York: Benjamin Press, 1988.
17. G. Rieke. Detection of Light: From the Ultraviolet to the Submillimeter. Cambridge, UK: Cambridge University Press, 2003.
18. M. Hercher. "The Spherical Mirror Fabry–Perot Interferometer". Appl. Opt. 1968. 7(5): 951–966.
19. S.A. Goldstein, J.P. Walters. "A Review of Considerations for High-Fidelity Imaging of Laboratory Spectroscopic Sources—I". Spectrochim. Acta, Part B. 1976. 31(4): 201–220.
20. S.A. Goldstein, J.P. Walters. "A Review of Considerations for High-Fidelity Imaging of Laboratory Spectroscopic Sources—II". Spectrochim. Acta, Part B. 1976. 31(5): 295–316.
21. R.L. McCreery. Raman Spectroscopy for Chemical Analysis. New York: John Wiley and Sons, 2000.
22. Oklahoma State University. Seidel Aberrations I. https://www.youtube.com/watch?v=wzEQX1tMLdY [accessed Jun 10 2017].
23. Ocean Optics. Spark-VIS Ultracompact Visible Spectral Sensor. http://oceanoptics.com/product/spark-vis/ [accessed Jan 1 2016].
24. D.L. Miller, A. Scheeline. "A Computer Program for the Collection, Reduction, and Analysis of Echelle Spectra". Spectrochim. Acta, Part B. 1993. 48(8): E1053–E1062.
25. A.T. Zander, R.-L. Chien, C.B. Cooper, P.V. Wilson. "An Image-Mapped Detector for Simultaneous ICP-AES". Anal. Chem. 1999. 71(16): 3332–3340.
26. M.J. Pelletier. "Raman Spectroscopy Using an Echelle Spectrograph with CCD Detection". Appl. Spectrosc. 1990. 44(10): 1699–1705.
27. J. Zhang, M. Yang, X. Puyang, Y. Fang, et al. "Two-Dimensional Direct-Reading Fluorescence Spectrograph for DNA Sequencing by Capillary Array Electrophoresis". Anal. Chem. 2001. 73(6): 1234–1239.
28. Princeton Instruments. IsoPlane Imaging Spectrographs. http://www.princetoninstruments.com/products/IsoPlane [accessed Jun 21 2017].
29. T.M. Niemczyk, G.W. Gobeli. "Stigmatic Flat Focal Field Spectrograph". Proc. SPIE. 1990. 1318: 33–43.
30. X. Prieto-Blanco, H. González-Nuñez, R. de la Fuente. "Off-Plane Anastigmatic Imaging in Offner Spectrometers". J. Opt. Soc. Am. A. 2011. 28(11): 2332–2339.
31. H. González-Nuñez, X. Prieto-Blanco, R. de la Fuente. "Pupil Aberrations in Offner Spectrometers". J. Opt. Soc. Am. A. 2012. 29(4): 442–449.
32. X. Prieto-Blanco, R. de la Fuente. "Compact Offner-Wynne Imaging Spectrometers". Opt. Commun. 2014. 328: 143–150.
33. E.A. Volkers, J. Bulthuis, S.R. Stolte, R. Jost, et al. "Vibronic Spectrum of $^{15}N_2^{16O}$ between 415 and 440 nm". J. Mol. Spectrosc. 2007. 245(1): 1–7.
34. L.L. Burton, M.W. Blades. "Influence of Instrumental Broadening on Lineshapes Detected by PMT and Photodiode Array Detectors". Spectrochim. Acta, Part B. 1987. 42(3): 513–519.
35. Excelitas Technologies. Datasheet, Photon Detection P-Series CCD Sensors Linear Photodiode Array Imager. http://www.excelitas.com/downloads/P-Series CCD Sensors.pdf [accessed Jun 21 2017].
36. R. Widenhorn, M.M. Blouke, A. Weber, A. Rest, et al. "Temperature Dependence of Dark Current in a CCD". Proc. SPIE 4669, Sensors and Camera Systems for Scientific, Industrial, and Digital Photography Applications III. 2002. 193 (April 26, 2002); doi:10.1117/12.463446. Pp. 193–201.
37. J. James. Spectrograph Design Fundamentals. Cambridge, UK: Cambridge University Press, 2007.
38. W.R. McKinney, C. Palmer. "Numerical Design Method for Aberration-Reduced Concave Grating Spectrometers". Appl. Opt. 1987. 26(15): 3108–3118.
39. C. Palmer. "Theory of Second-Generation Holographic Diffraction Gratings". J. Opt. Soc. Am. A. 1989. 6(8): 1175–1188.
40. Newport Corporation. Diffraction Grating Specification Sheet. http://www.gratinglab.com/Products/Product_Tables/Efficiency/Efficiency.aspx?catalog=53-*-172R [accessed Jun 21 2017].
41. R. Siegel, J.R. Howell. Thermal Radiation Heat Transfer.
42. W.G. Fastie. "Image Forming Properties of the Ebert Monochromator". J. Opt. Soc. Am. 1952. 42(9): 647–651.
43. W.G. Fastie. "A Small Plane Grating Monochromator". J. Opt. Soc. Am. 1952. 42(9): 641–647.
44. A. Arrak. "Focal Curve and Performance of the Spectrograph. I. The Method of Separation of Beams". Spectrochim. Acta. 1959. 15: 1003–1014.
45. The Engineering Toolbox, Coefficients of Linear Thermal Expansion. http://www.engineeringtoolbox.com/linear-expansion-coefficients-d_95.html [accessed Jan 28 2017].